Amplified Trace Gas Removal in the Troposphere

Andreas Hofzumahaus, *et al.*

Science **324**, 1702 (2009);
DOI: 10.1126/science.1164566

Science (print ISSN 0036-8075; online ISSN 1095-9203) is published weekly, except the last week in December, by the American Association for the Advancement of Science, 1200 New York Avenue NW, Washington, DC 20005.

11. R. H. Gammon, R. C. Stern, M. E. Lesk, B. G. Wicke, W. Klemperer, *J. Chem. Phys.* **54**, 2136 (1971).
12. The advantage of using metastable CO in the present experiments is that these molecules are prepared with a pulsed laser at a well-defined time and at a well-defined position in a single quantum state with the appropriate Stark shift. By detecting the Auger electrons when the metastable CO molecules impact on the Au surface, the full arrival-time distribution of the molecules can be recorded in a single pulse, and the schemes to manipulate the longitudinal phase-space distribution demonstrated in Fig. 3, for instance, can be rapidly tested and optimized. Even though the detection efficiency for metastable CO is not as good now as it can be for ionization detection, the multiplex nature of the trap-loading and detection scheme already enables us to detect down to one metastable CO molecule per hundred traps on the chip.
13. J. J. Gilijamse *et al.*, *J. Chem. Phys.* **127**, 221102 (2007).
14. S. Y. T. van de Meerakker, N. Vanhaecke, M. P. J. van der Loo, G. C. Groenenboom, G. Meijer, *Phys. Rev. Lett.* **95**, 013003 (2005).
15. W. C. Campbell, G. C. Groenenboom, H.-I. Lu, E. Tsikata, J. M. Doyle, *Phys. Rev. Lett.* **100**, 083003 (2008).
16. J. D. Weinstein, K. G. Libbrecht, *Phys. Rev. A* **52**, 4004 (1995).
17. E. A. Hinds, I. G. Hughes, *J. Phys. D Appl. Phys.* **32**, R119 (1999).
18. We acknowledge the help of B. G. Sartakov in the calculation of the hyperfine structure of ^{13}CO and the design of the electronics by G. Heyne, V. Platschkowski, and T. Vetter. This work has been funded by the European Community's Seventh Framework Program FP7/2007-2013 under grant agreement 216 774.

27 March 2009; accepted 26 May 2009
10.1126/science.1175975

Amplified Trace Gas Removal in the Troposphere

Andreas Hofzumahaus,[1] Franz Rohrer,[1]* Keding Lu,[1,2] Birger Bohn,[1] Theo Brauers,[1] Chih-Chung Chang,[3] Hendrik Fuchs,[1] Frank Holland,[1] Kazuyuki Kita,[4] Yutaka Kondo,[5] Xin Li,[1,2] Shengrong Lou,[1,6] Min Shao,[2] Limin Zeng,[2] Andreas Wahner,[1] Yuanhang Zhang[2]*

The degradation of trace gases and pollutants in the troposphere is dominated by their reaction with hydroxyl radicals (OH). The importance of OH rests on its high reactivity, its ubiquitous photochemical production in the sunlit atmosphere, and most importantly on its regeneration in the oxidation chain of the trace gases. In the current understanding, the recycling of OH proceeds through HO_2 reacting with NO, thereby forming ozone. A recent field campaign in the Pearl River Delta, China, quantified tropospheric OH and HO_2 concentrations and turnover rates by direct measurements. We report that concentrations of OH were three to five times greater than expected, and we propose the existence of a pathway for the regeneration of OH independent of NO, which amplifies the degradation of pollutants without producing ozone.

The central role of hydroxyl radicals (OH) in atmospheric chemistry was recognized by Levy in the early 1970s (*1*). Since then it has become more and more evident how OH radicals govern the degradation processes of air pollutants. OH radicals are short-lived (<1 s), and their formation and loss must be essentially balanced. OH is primarily formed through the photolysis of ozone, nitrous acid, and hydrogen peroxide and is consumed by a multitude of reactions with trace gases that can be oxidized. In this way, OH controls the removal of most atmospheric pollutants such as carbon monoxide (CO) and volatile organic compounds (VOCs). The OH reactions with CO and VOCs produce hydroperoxy (HO_2) and organic peroxy (RO_2) radicals, respectively. In continental air, with nitrogen oxides (NO_x) present, RO_2 is converted to HO_2 through reaction with NO. HO_2 further reacts with NO, thereby recycling OH. The ultimate loss of OH is the reaction with NO_2, forming nitric acid. These are the key processes that are believed to determine the self-cleaning ability of the troposphere (*2*, *3*). OH recycling enhances the efficiency of atmospheric oxidation, even at moderate NO concentrations. As a side effect, reactions of HO_2 or RO_2 with NO form NO_2, which produces ozone upon photolysis. This is the generally accepted, exclusive mechanism for the photochemical formation of ozone in the troposphere (*4*). OH formation through photolysis, HO_2 to OH recycling with NO, and OH loss with NO_2 have been established through a small number of well-understood reactions. In contrast, OH reactions with VOCs and the subsequent organic radical reactions are diverse and introduce enormous complexity into tropospheric chemistry, which is far from being fully explored (*5*, *6*).

The current understanding of tropospheric OH chemistry has been tested in a number of field campaigns, where the concentrations of OH and trace gases and meteorological parameters were observed simultaneously (*7*). However, OH observations are still too sparse, owing to the difficulty of measuring its extremely small and highly variable concentration, to provide a conclusive picture of the photochemistry in the entire troposphere (*8*–*10*). More experimental studies in different chemical environments are necessary to explore the various factors influencing the self-cleaning capability of the atmosphere. In this paper, we present concentration measurements of OH and HO_2 radicals in China (*11*), together with simultaneously measured mixing ratios of atmospheric trace gases and photolysis frequencies (*12*) (fig. S1). Complementary to direct measurements of VOCs, we also measured the total OH reactivity, k'_{OH}, corresponding to the inverse chemical lifetime of OH (*13*, *14*). Our measurements were part of an intense field campaign in a rural area, about 60 km NW of Guangzhou City, in the heavily populated Pearl River Delta (PRD) (*12*).

The diurnal dependences of the measured OH and HO_2 concentrations and k'_{OH} are shown

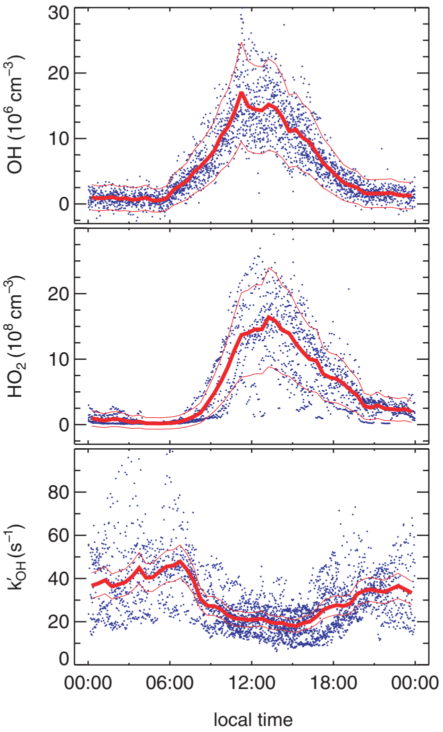

Fig. 1. Diurnal variation of OH, HO_2, and k'_{OH} near Guangzhou in the PRD, China, between 5 and 25 July 2006. Blue symbols denote individual data, and the thick red line the half-hourly mean diurnal profile. The enclosing thin red lines represent the maximum data variability caused by the measurement instrument (about 46% at noon), calculated as the sum of the 2σ measurement precision and the 2σ variability of its calibration. Campaign average calibration factors were used to convert measured OH and HO_2 signals into ambient concentrations.

---

[1] Forschungszentrum Jülich, Institut für Chemie und Dynamik der Geosphäre–2: Troposphäre, 52425 Jülich, Germany. [2] College of Environmental Sciences and Engineering, Peking University, Beijing 100871, China. [3] Research Center for Environmental Changes, Academic Sinica, Taipei, China. [4] Faculty of Science, Ibaraki University, Ibaraki 310-8512, Japan. [5] Research Center for Advanced Science and Technology, University of Tokyo, Tokyo 153-8904, Japan. [6] School of Environmental Science and Technology, Shanghai Jiaotong University, Shanghai 200240, China.

*To whom correspondence should be addressed. E-mail: f.rohrer@fz-juelich.de (F.R.); yhzhang@pku.edu.cn (Y.Z.)

in Fig. 1. The scatter of individual data points at a given time of day is caused by instrumental error (envelope lines in Fig. 1) and the variability of atmospheric conditions. In the following, we refer to the mean diurnal profiles, which have an improved measurement precision for OH and HO_2 of about 5%. The most striking feature is the high average OH concentration of 15×10^6 cm^{-3} around noon, which is maintained despite a large OH reactivity of about 20 s^{-1}. Most of that OH reactivity can be attributed to the heavy load of VOCs, with a substantial amount of isoprene, whereas only about 20% is explained by measured CO and NO_x [supporting online material (SOM) text]. Another remarkable feature is the very high noontime HO_2 concentration, yielding an HO_2/OH ratio of about 100, which is normally found only in clean air at low concentrations of NO_x (*15*). Although the air at the PRD was rich in VOCs, the level of NO at noon was surprisingly low, with an average of about 200 parts per trillion (ppt).

Figure 2A presents the total OH loss rate, calculated as the product of the OH concentration, [OH], and k'_{OH}. The high [OH] coinciding with a large OH reactivity at noontime causes a loss rate of approximately 40 parts per billion (ppb)/hour, which corresponds to an equivalent turnover in CO and VOCs. These values exceed recent observations in Mexico City (*16*) by a factor of 1.7. To maintain a steady state in [OH] requires an equally large OH production rate. We find that at the PRD, the OH production from all known sources cannot balance the large consumption rate of OH when NO drops to low values in the late morning (Fig. 2B). For instance, at noontime the OH recycling rate through the NO + HO_2 reaction is about 8 ppb/hour (Fig. 2A) and the primary OH production is 4 ppb/hour only (Fig. 2C). Apparently, the photochemical mix at the PRD maintains a hitherto unknown source of OH of about 28 ppb/hour, which is about two times larger than that of the known OH production processes displayed in Fig. 2 and sustains a highly efficient removal of trace gases by OH. This conclusion is based entirely on measurements and does not depend on modeled parameters.

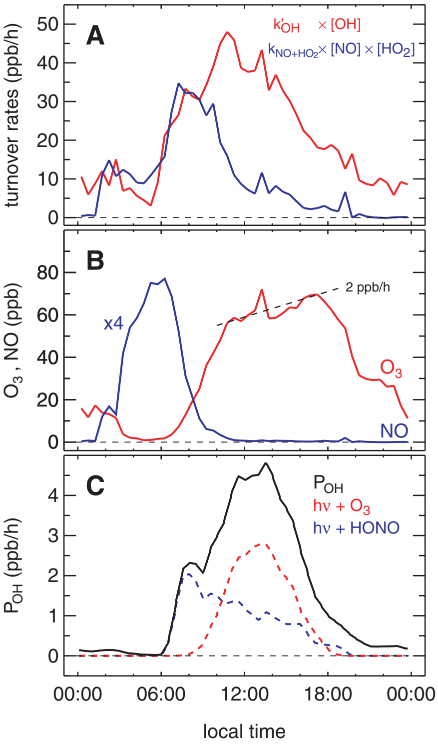

Fig. 2. Analysis of mean diurnal OH production and loss rates derived from measurements at the PRD in July 2006. (**A**) The red line denotes the total OH loss rate, the blue line the OH recycling rate from the reaction of HO_2 with NO, and (**C**) the black line the total primary OH production rate (P_{OH}) from photolysis and ozonolysis processes. The major contributions from the photolysis of ozone and HONO are shown by the red and blue dashed lines, respectively. (**B**) Mean diurnal profiles of ozone and NO.

Additionally, we performed chemical box-model calculations (*12*) for OH and HO_2, which are displayed in Fig. 3 as mean diurnal profiles, together with the experimental data. The model yields an excellent description of the measured HO_2 for the entire day, indicating that the ratio of the production to destruction rates of HO_2 is simulated correctly. Concentrations of OH, however, match only in the early morning to about 10:00; that is, as long as NO remains above 1 ppb. Thereafter, the measured [OH] is significantly larger than predicted by the model by a factor of 3 to 5 at low NO levels (<1 ppb). The discrepancy cannot be explained by the systematic experimental and modeling errors of 20 and 40%, respectively (fig. S6), and an experimental OH interference of the necessary magnitude is highly unlikely (SOM text). The measured OH reactivities are well described by the model during daytime (fig. S4). This and the failure of the model to reproduce the observed [OH] correctly is synonymous with our conclusion from Fig. 2, that the known OH sources are not enough to sustain the observed reaction rate of OH with pollutants.

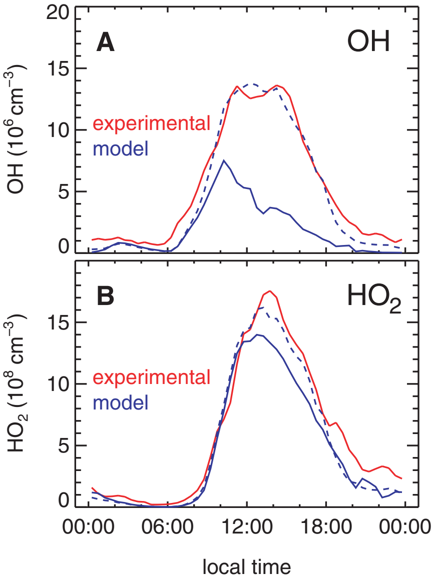

Fig. 3. Comparison of measured and modeled mean diurnal profiles of (**A**) OH and (**B**) HO_2. Red lines represent experimental data, blue solid lines the Regional Atmospheric Chemistry Mechanism (RACM) results (base case), and blue dashed lines the results from the extended RACM model with enhanced HO_2 and RO_2 recycling. The figure uses a subset of field campaign data, in which all required measurements are simultaneously available over full diurnal cycles.

In further simulations, we extended the model by various generic radical-production processes that might explain the measured diurnal variations of both OH and HO_2. Based on these model runs, we can exclude additional primary sources of OH or HO_2 to explain the observations. They would increase both species by a similar factor, because the partitioning of OH and HO_2 is largely maintained. An additional source in the model to match the measured OH would result in a significant overprediction of HO_2. Incidentally, the reaction of excited NO_2 with H_2O, a recently recognized new OH source (*17*), is too small to make a difference in our model results.

Additional recycling of peroxy radicals to OH is another way to increase the modeled [OH]. Peroxy reactions such as $RO_2 + HO_2 \rightarrow \alpha \times OH$ have been proposed to be a potentially significant source of atmospheric OH at low NO conditions (*10*, *18*). Laboratory studies provided α values up to 0.6 for specific RO_2 (*19*–*21*). Even at $\alpha = 1$ for all RO_2 species, this process can explain only 15 to 30% of the additionally required OH, because most RO_2 (70 to 80%) reacts with NO (100 to 200 ppt) rather than with HO_2 (up to 60 ppt; SOM text). Lelieveld *et al.* (*10*) explained unexpectedly high [OH] in an isoprene-rich, low-NO (~20 ppt) environment, assuming $\alpha = 2$ to 4 for the reaction of isoprene peroxy radicals. In contrast to the laboratory work, this requires additional photolysis of reaction products. Again, this hypothesis cannot explain our observations at the PRD, given the significantly larger rate of the competing RO_2 + NO reaction. Another possible path of HO_2 to OH by reaction with halogen oxides (BrO and IO) was observed in marine air at Cape Verde (*22*). This route can be discarded here as highly unlikely, because the required halogen oxide concentrations exceed all tropospheric observations, and no halogen sources were noted at the PRD (SOM text).

In order to reach the measured [OH] but maintain the level of observed HO_2, the mechanism needs to include reactions that as a net effect convert RO_2 to HO_2 and HO_2 to OH. The actual chemical mechanism of the proposed OH

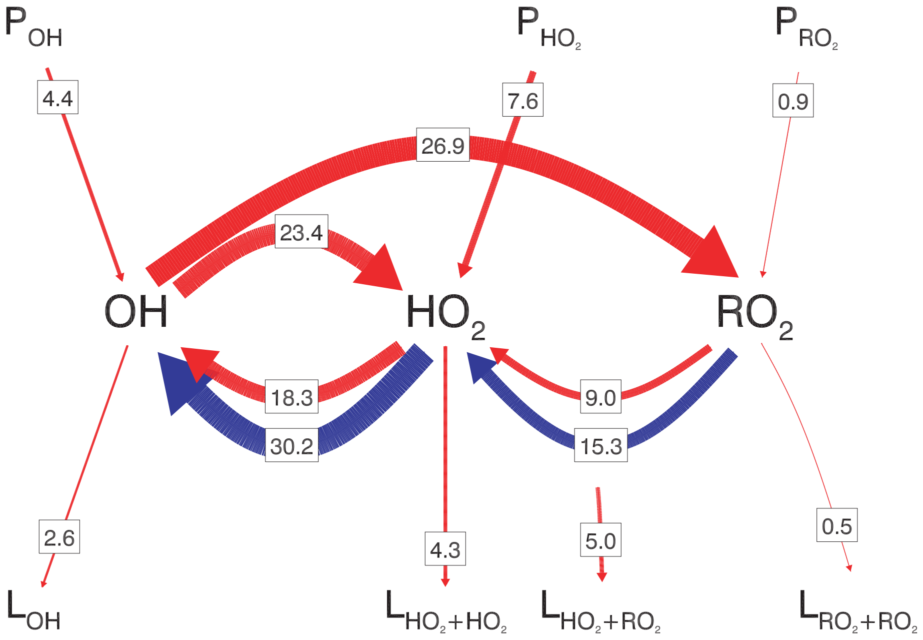

Fig. 4. Generic chart of the chemistry of tropospheric OH radicals. The arrows represent chemical processes which generate (P→), remove (→L), or interconvert (A→B) radicals. The width of the arrows scales with the reaction rates (in parts per billion per hour), given by the numbers in boxes, at 12:00 local time at Guangzhou in July 2006. Red arrows represent known reaction pathways of the RACM model and blue arrows the additional recycling processes needed to maintain the observed high [OH]. The total OH loss rate, $k'_{OH} \times [OH]$, corresponds to the sum of arrows $OH \rightarrow HO_2$, $OH \rightarrow RO_2$, and OH → LOH. The OH recycling by NO, $k_{HO_2+NO} \times [NO] \times [HO_2]$, is represented by the red arrow $HO_2 \rightarrow OH$.

recycling is not clear. In the most simple case, there could be two reactions, $RO_2 + X \rightarrow HO_2$ and $HO_2 + X \rightarrow OH$, both of similar rate, as in the case of the corresponding NO reactions. Another possibility would be reactions with several reactants, each of which makes a small contribution, summing up to a large OH source. Including the two reactions with a single reactant X as formulated above and assuming for X a reactive equivalent of 0.85 ppb of NO [obtained from an optimization (*12*)], the model is able to reproduce the mean diurnal cycles of both OH and HO_2 at high- and low-NO_x conditions during daytime surprisingly well (Fig. 3). The corresponding radical conversion rates at noon and in the afternoon are illustrated in Fig. 4 and fig. S7, respectively, quantifying the important role of the assumed recycling process for maintaining a high [OH].

In case of OH recycling with a single species X, a strong source of X would be required during the noon and afternoon hours. It could be direct emission, conversion from a large reservoir, or a recycling process of X. Steps toward the identification of the unknown OH recycling mechanism require further field and laboratory experiments to identify the reactions and chemical species involved, which are missing from current tropospheric chemistry models.

The existence of an additional radical-recycling mechanism has a potentially important implication for our ability to predict the photochemical formation of tropospheric ozone (*18*). In the current understanding, in which OH is recycled only by NO reactions, the oxidation of a CO or VOC molecule with OH can produce one or up to three ozone molecules, respectively (*23*). For a high turnover rate of 40 ppb/hour of OH as observed at the PRD at noontime (Fig. 2A), the classical mechanism would yield, with sufficient NO, a net production of ozone of about 60 ppb/hour. The observed trend of the mean diurnal ozone profile, however, is only 2 ppb/hour at noon and shortly thereafter (Fig. 2B). This suggests that the unknown radical-recycling process is not likely to produce much ozone, because the estimated loss by transport (<2 ppb/hour) cannot dissipate a potential net production of 60 ppb/hour (SOM text). If we run the extended model (Fig. 3) and assume that the proposed recycling mechanism does not form ozone, we calculate a chemical ozone increase of 7 ppb/hour, which is roughly in line with the observed ozone trend.

Unexplained high [OH] was observed previously in the presence of high VOC mixing ratios and at low to moderate NO_x levels in rural forested North America (*9*, *24*) and above the tropical rainforest in Surinam (*10*). In these regions, biogenic VOCs, mostly isoprene, are abundant and contribute significantly to the atmospheric OH reactivity, as in our observations at the PRD field site. Measured [OH] under clean air conditions (*25*) (low NO_x and low VOCs) and in highly polluted areas (*16*) (high NO_x and high VOCs), however, can be explained reasonably well by current models. Thus, the shortcoming of photochemistry models by underestimating tropospheric [OH], seems to apply only to low-NO_x and high-VOC regions, as encountered in the northern part of the PRD, and thus probably to large areas where a major portion of natural VOCs is emitted globally.

Current atmospheric chemistry models predict large formation of secondary pollutants such as ozone in strong correlation to trace gas degradation. Our observations suggest that the proposed recycling mechanism does not produce ozone but increases the stability of the [OH] and amplifies the oxidation capacity in the troposphere.

References and Notes

1. H. Levy II, *Science* **173**, 141 (1971).
2. D. H. Ehhalt, *Phys. Chem. Chem. Phys.* **1**, 5401 (1999).
3. G. P. Brasseur, R. G. Prinn, A. P. Pszenny, Eds., *Atmospheric Chemistry in a Changing World, Global Change—The IGAC Series* (Springer Verlag, Berlin, 2003).
4. S. C. Liu *et al.*, *J. Geophys. Res.* **92**, 4191 (1987).
5. B. Aumont, S. Szopa, S. Madronich, *Atmos. Chem. Phys.* **5**, 2497 (2005).
6. A. H. Goldstein, I. E. Galbally, *Environ. Sci. Technol.* **41**, 1514 (2007).
7. D. E. Heard, M. J. Pilling, *Chem. Rev.* **103**, 5163 (2003).
8. F. Rohrer, H. Berresheim, *Nature* **442**, 184 (2006).
9. X. R. Ren *et al.*, *J. Geophys. Res.* **113**, D05310 (2008).
10. J. Lelieveld *et al.*, *Nature* **452**, 737 (2008).
11. F. Holland, A. Hofzumahaus, R. Schäfer, A. Kraus, H. W. Pätz, *J. Geophys. Res.* **108**, 8246 (2003).
12. Information on measurement methods, modeling, and chemical conditions is available as supporting material on *Science* Online.
13. P. Di Carlo *et al.*, *Science* **304**, 722 (2004).
14. Y. Sadanaga, A. Yoshino, S. Kato, Y. Kajii, *Environ. Sci. Technol.* **39**, 8847 (2005).
15. D. J. Creasey, G. E. Evans, D. E. Heard, J. D. Lee, *J. Geophys. Res.* **108**, 4475 (2003).
16. T. R. Shirley *et al.*, *Atmos. Chem. Phys.* **6**, 2753 (2006).
17. S. Li, J. Matthews, A. Sinha, *Science* **319**, 1657 (2008).
18. J. A. Thornton *et al.*, *J. Geophys. Res.* **107**, 10.1029/2001JD000932 (2002).
19. A. S. Hasson, G. S. Tyndall, J. J. Orlando, *J. Phys. Chem. A* **108**, 5979 (2004).
20. M. E. Jenkin, M. D. Hurley, T. J. Wallington, *Phys. Chem. Chem. Phys.* **9**, 3149 (2007).
21. T. J. Dillon, J. N. Crowley, *Atmos. Chem. Phys.* **8**, 4877 (2008).
22. K. A. Read *et al.*, *Nature* **453**, 1232 (2008).
23. L. I. Kleinman *et al.*, *J. Geophys. Res.* **107**, 4733 (2002).
24. D. Tan *et al.*, *J. Geophys. Res.* **106**, 24407 (2001).
25. T. Brauers, M. Hausmann, A. Bister, A. Kraus, H.-P. Dorn, *J. Geophys. Res.* **106**, 7399 (2001).

26. We thank the PRiDe PRD 2006 campaign team (2002CB410801), especially L. J. Zhong, M. Hu, N. Takegawa, Y. Miyazaki, M. Koike, R. Häseler, and A. Oebel, for technical help and support at the field site, and J. L. Wang for help in the in situ measurement of VOCs. C.C. thanks Academic Sinica, Taiwan, for financial support of this work. Discussions with S. C. Liu and D. H. Ehhalt are gratefully acknowledged.

Supporting Online Material

www.sciencemag.org/cgi/content/full/1164566/DC1
Methods
SOM Text
Figs. S1 to S9
References

12 August 2008; accepted 21 May 2009
Published online 4 June 2009;
10.1126/science.1164566
Include this information when citing this paper.